

Supplementary Material: Implicit neural representation for change detection

Peter Naylor^{1†}, Diego Di Carlo¹, Arianna Traviglia², Makoto Yamada^{1,3} and Marco Fiorucci²

¹ RIKEN AIP, Kyoto, Japan `firstname.lastname@riken.jp`

² Istituto Italiano di Tecnologia, Venice, Italy `firstname.lastname@iit.it`

³ OIST, Okinawa, Japan `makoto.yamada@oist.jp`

We show in the Supplementary Material results of all the methods applied to each data configuration in Table A.1. We summarise all the possible architectures that we optimise from in Table A.2 and show an example model in Fig. A.1. In addition, we give the AUC plot between RFF, SIREN and no feature mapping in Fig. A.3. We show in Fig. A.2 the distribution of a typical Δz , mapped with the true labels and mapped with the predicted GMM labels. Finally, we show an additional samples of surface reconstruction, namely, the whole map in Fig. A.4, a medium size crop in Fig. A.5, another medium-field size crop in Fig. A.6 and a close field crop in Fig. A.7. In Fig. A.4, we also show where each crop was extracted from, including the one in the main text.

[†]Now at ESA/ESRIN, Φ -lab, Italy. `peter.naylor@esa.int`

Data	D	D+TVN	S	S+TD	S+TVN	S+TD+TVN	Data	D	D+TVN	S	S+TD	S+TVN	S+TD+TVN
(1)	90.12	88.61	96.99	92.00	95.47	96.64	(1)	23.73	23.65	21.14	19.36	37.22	35.26
(2)	97.21	97.10	98.68	98.39	98.68	98.82	(2)	38.24	37.22	46.72	45.12	45.22	48.72
(3)	91.04	85.07	95.53	95.72	96.40	96.00	(3)	26.27	20.76	31.75	30.31	33.11	31.49
(4)	89.93	87.34	95.63	95.71	96.12	82.96	(4)	21.24	20.53	35.19	32.34	33.54	23.23
(5)	93.06	92.87	97.80	97.73	97.42	86.52	(5)	20.35	19.92	31.32	26.35	37.97	17.24
Avg	92.27	90.20	96.92	95.91	96.82	92.19	Avg	25.97	24.42	33.22	30.69	37.41	31.19

(a) AUC for no feature mapping							(b) IoU for no feature mapping						
Data	D	D+TVN	S	S+TD	S+TVN	S+TD+TVN	Data	D	D+TVN	S	S+TD	S+TVN	S+TD+TVN
(1)	98.11	98.10	98.18	98.04	98.43	98.58	(1)	50.12	44.67	52.49	54.73	55.86	49.67
(2)	98.18	98.19	98.34	98.09	98.26	98.67	(2)	57.38	59.32	56.45	60.33	61.16	59.52
(3)	97.62	97.76	97.48	97.43	98.05	97.96	(3)	46.54	43.16	51.87	53.99	46.94	53.33
(4)	97.63	97.59	97.62	97.66	98.14	97.93	(4)	48.62	49.69	51.38	53.40	51.10	53.99
(5)	97.54	97.92	97.64	96.83	98.04	97.73	(5)	42.55	43.15	42.95	40.55	43.25	47.17
Avg	97.82	97.91	97.85	97.61	98.18	98.18	Avg	49.04	48.00	51.03	52.60	51.66	52.74

(c) AUC for RFF							(d) IoU for RFF						
Data	D	D+TVN	S	S+TD	S+TVN	S+TD+TVN	Data	D	D+TVN	S	S+TD	S+TVN	S+TD+TVN
(1)	97.80	97.45	97.74	97.49	98.04	97.77	(1)	41.47	38.45	40.14	38.12	43.07	35.99
(2)	98.13	97.79	98.44	98.24	98.30	97.93	(2)	52.55	44.40	53.97	49.08	48.43	43.95
(3)	97.02	97.45	97.55	96.41	96.27	96.60	(3)	40.84	39.93	38.57	42.91	38.36	37.23
(4)	97.16	97.95	96.99	97.48	97.21	97.40	(4)	37.77	38.33	39.01	37.25	41.07	40.13
(5)	97.59	97.74	97.54	93.26	97.37	97.48	(5)	38.65	37.96	40.47	29.57	35.53	37.44
Avg	97.54	97.68	97.65	96.58	97.44	97.44	Avg	42.26	39.81	42.43	39.39	41.29	38.95

(e) AUC for SIREN							(f) IoU for SIREN						
Data	D	D+TVN	S	S+TD	S+TVN	S+TD+TVN	Data	D	D+TVN	S	S+TD	S+TVN	S+TD+TVN
(1)	97.80	97.45	97.74	97.49	98.04	97.77	(1)	41.47	38.45	40.14	38.12	43.07	35.99
(2)	98.13	97.79	98.44	98.24	98.30	97.93	(2)	52.55	44.40	53.97	49.08	48.43	43.95
(3)	97.02	97.45	97.55	96.41	96.27	96.60	(3)	40.84	39.93	38.57	42.91	38.36	37.23
(4)	97.16	97.95	96.99	97.48	97.21	97.40	(4)	37.77	38.33	39.01	37.25	41.07	40.13
(5)	97.59	97.74	97.54	93.26	97.37	97.48	(5)	38.65	37.96	40.47	29.57	35.53	37.44
Avg	97.54	97.68	97.65	96.58	97.44	97.44	Avg	42.26	39.81	42.43	39.39	41.29	38.95

Table A.1. Performance each data configuration for AUC and IoU (in %). D denotes the model with two DNN given by equation (1) and S the model with a single DNN given by equation (2).

Models								
default	default-BN	default-L	skip-double	skip-L-double	skip-XL-double	skip-ten	skip-ten-only	skip-twenty
Input $\gamma(\mathbf{v})$								
		FC-1024		FCS-1024 ($\times 2$)	FCS-1024 ($\times 4$)			
		FC-512	FCS-512 ($\times 2$)	FCS-512 ($\times 2$)	FCS-512 ($\times 4$)	FCS-512 ($\times 10$)		
FC-256	FC-256 + BN	FC-256	FCS-256 ($\times 2$)	FCS-256 ($\times 2$)	FCS-256 ($\times 3$)	FCS-256	FCS-256 ($\times 10$)	FCS-256 ($\times 20$)
FC-128	FC-128 + BN	FC-128	FCS-128	FCS-128 ($\times 2$)	FCS-128 ($\times 2$)	FCS-128		FCS-128 ($\times 2$)
FC-64	FC-64 + BN	FC-64	FCS-64	FCS-64 ($\times 2$)	FCS-64 ($\times 2$)	FCS-64		FCS-64 ($\times 2$)
Linear mapping to a 1 dimensional output								

Table A.2. Neural Network models. FC denotes fully connected layers with a given activation. BN-denotes batch normalisation. FCS denotes fully connected layers with a skip layer. For the transition when downsampling the dimension for fully connected skip layers, we add a simple FC that maps from one dimension to the other.

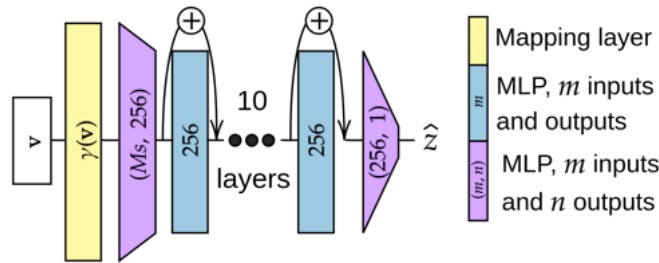


Figure A.1. Neural network model, 'skip-ten-only'.

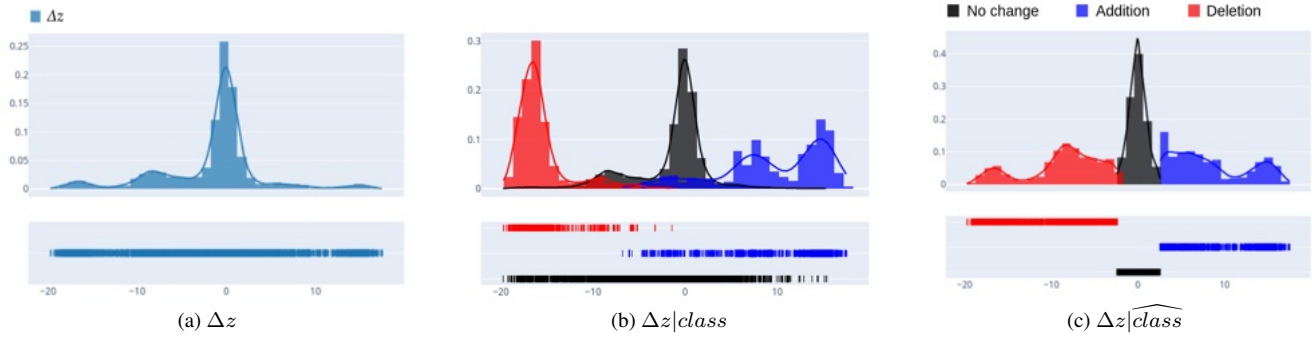


Figure A.2. Distribution of Δz and with predicted and true class label. This distribution was computed on a small subset with a single DNN (i.e. equation (1)) with the RFF and no regularisation.



Figure A.3. AUC results (in %) for different feature mapping methods for every LiDAR airborne simulated dataset.

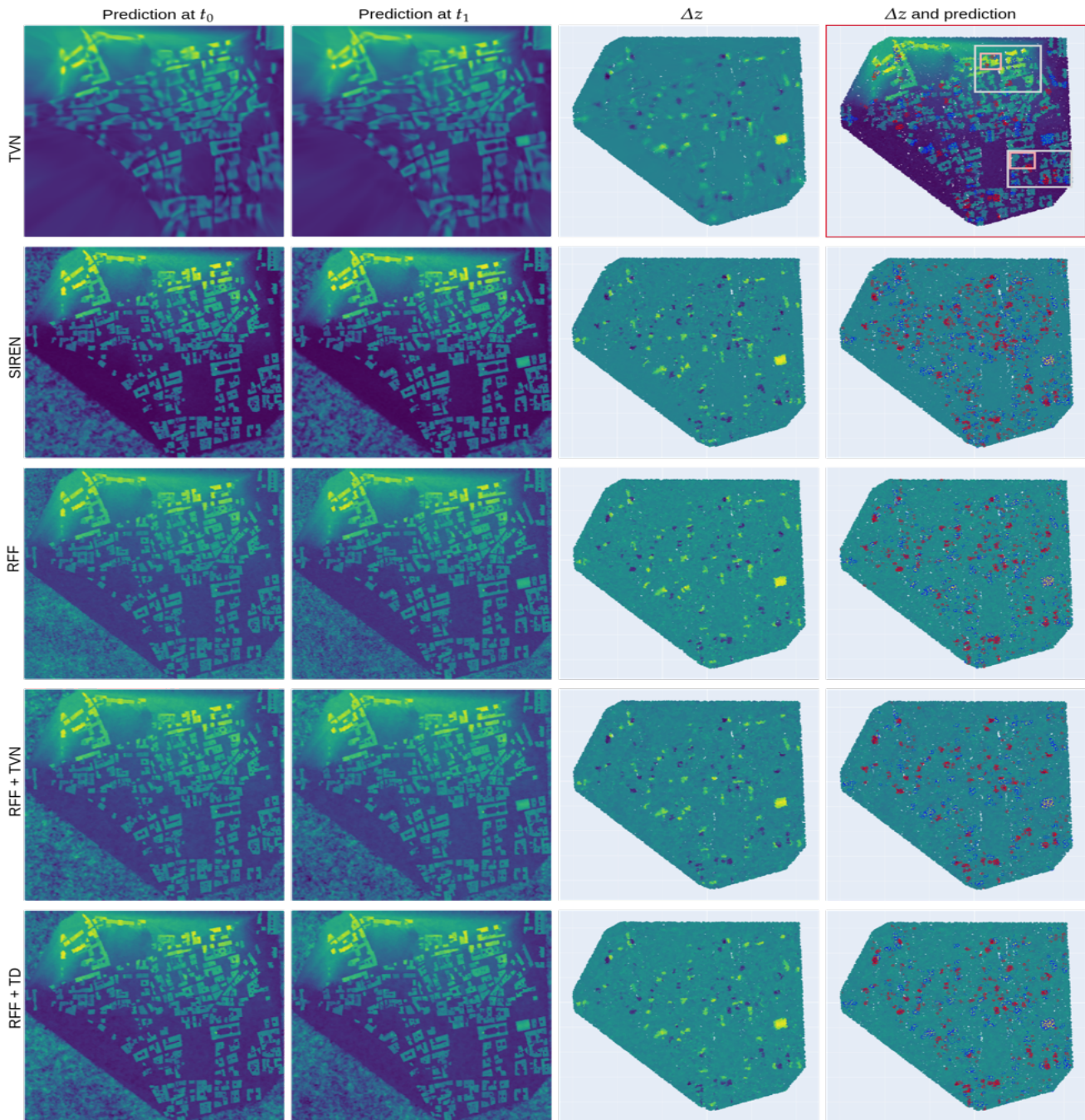


Figure A.4. Visualisation of the whole map where in each row we show a different method comprising a single DNN. In the two first columns, we have the reconstruction of the surface along a regular grid for timestamp t_0 and t_1 . In the third column, we show the difference Δz on the support of \mathcal{X}_1 and in the fourth column we overlay these difference with the predicted labels from the GMM. Each column shows a different method. In the first row and in the last column we show the true cloud point overlaid with the ground truth. In addition, we show where the previous crops and sub-crops were extracted from in white and light red. To compare fairly, we range the color map from dark purple, 160m altitude, to yellow, 245m, for the first two rows and from -30m to 30m for the visualisation of Δz .

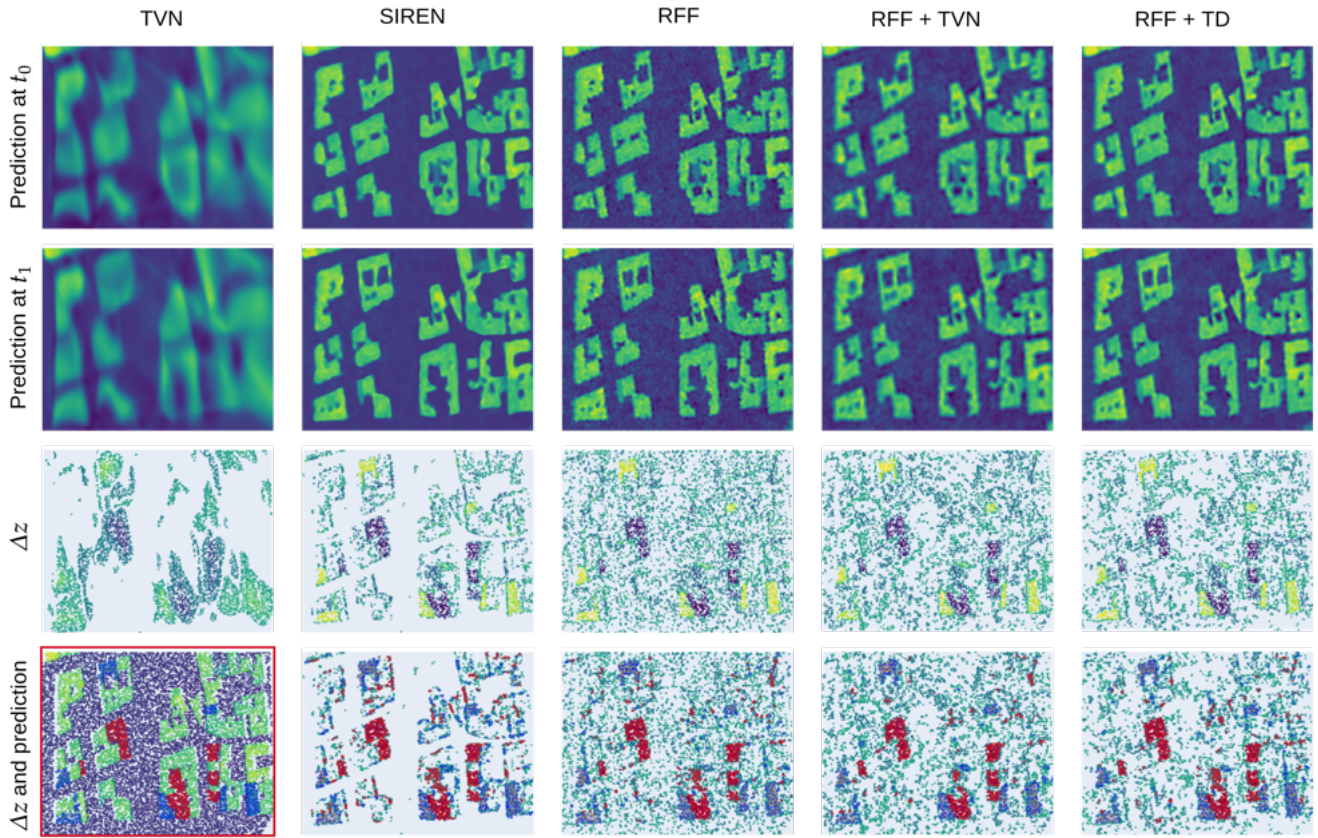


Figure A.5. Visualisation of a crop number 1 where in each column we show a different method comprising a single DNN applied. In the two first rows, we have the reconstruction of the surface along a regular grid for timestamp t_0 and t_1 . In the third row, we show the difference Δz on the support of \mathcal{X}_1 and in the fourth row we overlay these difference with the predicted labels from the GMM, we filter out points where $|\Delta z| < 2$. Each column shows a different method. In the final row and in the first column we show the true cloud point overlaid with the ground truth. To compare fairly, we range the color map from dark purple, 160m altitude, to yellow, 245m, for the first two rows and from -30m to 30m for the visualisation of Δz .

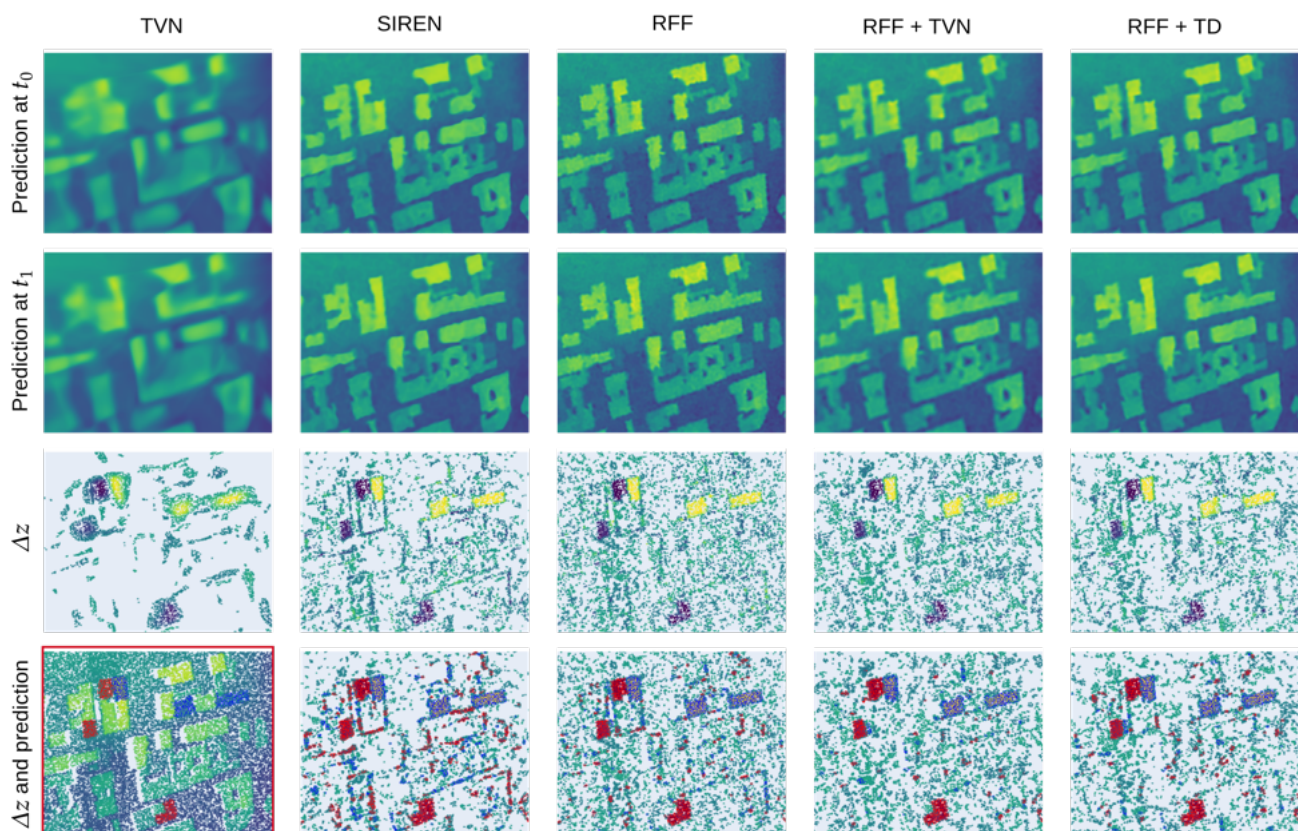


Figure A.6. Visualisation of a crop number 2 where in each column we show a different method comprising a single DNN applied. In the two first rows, we have the reconstruction of the surface along a regular grid for timestamp t_0 and t_1 . In the third row, we show the difference Δz on the support of \mathcal{X}_1 and in the fourth row we overlay these difference with the predicted labels from the GMM, we filter out points where $|\Delta z| < 2$. Each column shows a different method. In the final row and in the first column we show the true cloud point overlaid with the ground truth. To compare fairly, we range the color map from dark purple, 160m altitude, to yellow, 245m, for the first two rows and from -30m to 30m for the visualisation of Δz .

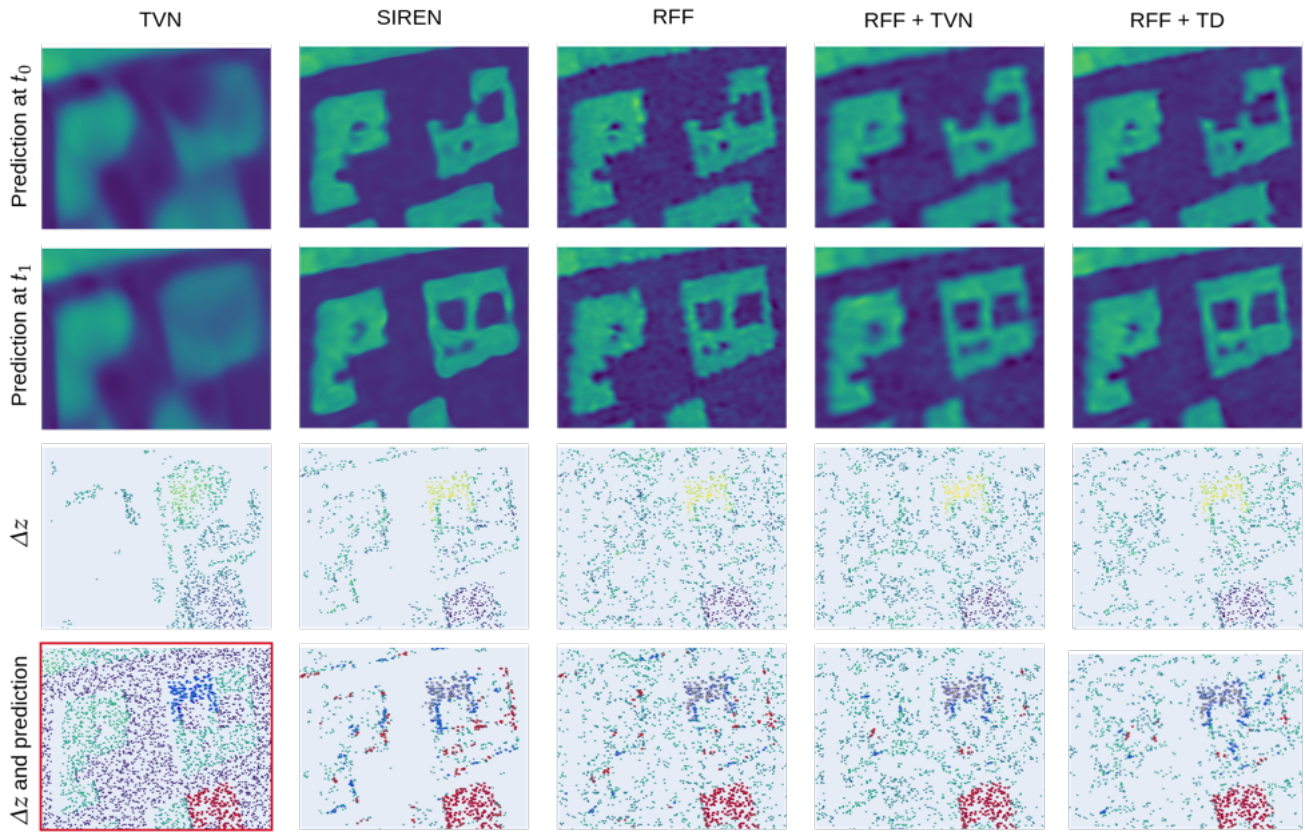


Figure A.7. Visualisation of a sub-crop number 1 of crop number 1, where in each column we show a different method comprising a single DNN applied. In the two first rows, we have the reconstruction of the surface along a regular grid for timestamp t_0 and t_1 . In the third row, we show the difference Δz on the support of \mathcal{X}_1 and in the fourth row we overlay these difference with the predicted labels from the GMM, we filter out points where $|\Delta z| < 2$. Each column shows a different method. In the final row and in the first column we show the true cloud point overlaid with the ground truth. To compare fairly, we range the color map from dark purple, 160m altitude, to yellow, 245m, for the first two rows and from -30m to 30m for the visualisation of Δz .